·封面文章·

拉曼光谱技术在肿瘤诊断上的应用研究进展

祁亚峰，刘宇宏*，刘大猛

清华大学机械工程系摩擦学国家重点实验室，北京　100084

摘要　肿瘤是一种严重威胁我国居民生命健康的重大疾病。现有的肿瘤诊断方式存在诊断时间长、创伤严重和误判率高等问题，且严重依赖于医生的主观经验。因此，研究出具有智能属性的肿瘤诊断技术对于提升我国的肿瘤诊断水平具有重要意义。拉曼光谱技术是一种无需标记的光学技术，在肿瘤的良恶性判别、肿瘤的亚型分类、切片病理诊断、原位近实时成像等方面被广泛应用。此外，人们将拉曼光谱与人工智能结合发展了具有智能属性的诊断方式。本文主要综述了近三年拉曼光谱技术在各种类型肿瘤诊断上的研究进展，主要从常规拉曼光谱诊断、拉曼成像诊断与探头结合光谱诊断三方面展开介绍，并对拉曼光谱技术在肿瘤诊断中的应用前景进行了展望。

关键词　医用光学；肿瘤诊断；拉曼光谱；拉曼成像；智能诊断

中图分类号　O657.37　　　　**文献标志码**　A　　　　　　　　**doi**：10.3788/LOP57.220001

Research Progress on Application of Raman Spectroscopy in Tumor Diagnosis

Qi Yafeng, Liu Yuhong*, Liu Dameng

State Key Laboratory of Tribology, Department of Mechanical Engineering, Tsinghua University, Beijing 100084, China

Abstract　Tumors are a major disease that seriously threaten the life and health of Chinese residents. Existing tumor diagnosis methods heavily rely on the subjective experience of doctors and include many issues, such as prolonged diagnosis, severe trauma, and high misdiagnosis rate. Therefore, it is crucial to develop a tumor diagnosis technology with intelligent properties to improve the level of diagnosing tumors in China. Raman spectroscopy is a label-free optical technique used for diagnosing benign and malignant tumors, classifying tumor subtypes, pathological diagnosis of biopsy, and *in situ* near-real-time imaging. Moreover, Raman spectroscopy combined with artificial intelligence has led to an intelligent diagnostic method. In this paper, the research progress of Raman spectroscopy for diagnosing various tumor types over the past three years was reviewed. Furthermore, three main aspects of the conventional Raman spectrum, Raman imaging, and probe diagnoses combined with the spectrum were introduced, and the prospect of Raman spectroscopy in the diagnosis of tumors in the future was discussed.

Key words　medical optics; tumor diagnosis; Raman spectroscopy; Raman imaging; intelligent diagnosis

OCIS codes　170.3880; 170.5660; 170.6510

1　引　　言

　　肿瘤作为严重威胁我国居民生命健康的重大疾病，是我国居民死亡的主要原因之一[1-2]。数据显示：2015 年恶性肿瘤占我国居民全部死因的23.91%，且近十几年来恶性肿瘤的发病率和死亡率均呈持续上升态势[3]。由于缺乏肿瘤筛查手段以及对"早发现、早诊断、早治疗"策略认知的不足，我国肿瘤患者五年生存率仅为 30.9%，远低于欧美国家。目前，肿瘤的三种主要检测方法为肿瘤标志物检测、影像学诊断和组织病理学诊断。肿瘤标志物检测[4-5]是从分子生物学角度进行早期肿瘤监测的

一种方法,易受个体差异及某些良性疾病的影响。影像诊断方式[6-9]在临床上通常只作为辅助手段,因为其仅可对肿瘤的形状和性质进行初期判别,无法准确分辨肿瘤的性质。组织病理学诊断[10-12]是肿瘤诊断临床应用上的"金标准",该方法从组织和细胞尺度上进行肿瘤的诊断。组织病理学是一门非常复杂的学科,要求检测人员具有丰富的经验,对检测人员的专业性要求较高,且诊断的时效性差,属于有创的诊断方式。

综上所述,临床肿瘤诊断的现有方法存在诊断时间长、创伤严重和误判率高等问题,且严重依赖于医生的主观经验。因此,研发出一种新型、快速、无创、高灵敏度的诊断技术,对于我国居民的生命健康保障具有十分重要的意义。

组织的癌变是一个十分复杂的过程,涉及到核酸、蛋白质等生物大分子含量和结构的变化。正常组织与癌变组织、不同时期癌变组织的形态和成分构成在细胞和分子水平上都存在一定差异。光谱技术具有极高的精确度和灵敏度,可获得分子的指纹图谱信息,可为癌变组织的精准、无创性检测提供一条可行性途径。由印度科学家 C. V. 拉曼(Raman)于 1928 年提出的拉曼光谱技术[13]具有特异性、无需标记等优点,可以通过拉曼峰频移的位置分析物质的生化组成,因而在肿瘤组织性质的判断上有很大的应用空间。拉曼光谱成像技术是一种利用光与物质的相互作用来研究分子结构与动态特征的技术,该技术可以获取光的发射、吸收、散射光谱信息以及三维空间成像信息,还可以获得研究对象的几何形态、分子结构及动态特性等信息,有望被应用于肿瘤组织的快速成像,从而可以根据成像结果的形态学及色彩变化来诊断肿瘤的亚型及类型。

目前,拉曼光谱技术及拉曼成像技术已被应用于多种肿瘤的诊断上。本文综述了近三年拉曼光谱技术在各种肿瘤诊断上的应用研究进展,主要从常规拉曼光谱诊断、拉曼成像诊断与探头结合光谱诊断三方面展开介绍,并对今后拉曼光谱技术在肿瘤诊断中的应用前景进行了展望。

2 拉曼光谱与拉曼成像技术简介

一束单色光入射到样品上之后,存在三种去向:一部分光被透射,一部分光被吸收,一部分光被散射。散射光中的大部分与入射光具有相同的波长(颜色),这种散射方式被称为瑞利散射(Rayleigh

scattering)。然而,有极小一部分(大约 $1/10^9$)散射光的波长(颜色)与入射光不同,其波长变化是由样品(即"散射物质")的化学结构决定的,这部分散射被称为拉曼散射(Raman scattering)。拉曼散射根据反射光波长($\lambda_{scatter}$)与入射光波长($\lambda_{incident}$)的相对大小又分为斯托克斯(Stokes)拉曼散射($\lambda_{scatter} > \lambda_{incident}$)和反斯托克斯(anti-Stokes)拉曼散射($\lambda_{scatter} < \lambda_{incident}$)。通常,拉曼散射强度约为入射光强度的 $10^{-8} \sim 10^{-6}$,而且反斯托克斯拉曼散射强度低于斯托克斯拉曼散射强度[14]。

拉曼谱图通常由一定数量的拉曼峰构成,每个拉曼峰代表了相应的拉曼散射光的波长位置和强度,同时对应一种特定的分子键振动,既包括单一的化学键振动[15],如 C—C、C═C 、C—H、N—O 等,也包括由数个化学键组成的基团的振动,如苯环的呼吸振动、多聚物长链的振动、晶格的振动等。拉曼谱线的数目、位移值的大小和谱带的强度等只与分子结构有关,不受入射光频率的影响。由于水的拉曼散射信号极弱,不会对生物分子的特征信号峰产生干扰,因此拉曼光谱可用于固体、粉末、液体、胶体、软膏、气体等生物分子结构的原位分析,可对无机材料、有机材料、生物材料进行分析,也可对纯物质、混合物、溶液进行处理,且不需进行任何预处理,可以避免预处理过程对信号的破坏。

自发拉曼散射信号的强度弱、抗干扰能力差,在实际应用中通常需要很长的积分时间才能获得信噪比可以接受的光谱,不利于光谱采集和快速成像。而且,生物样品中较强的荧光背景也会进一步降低拉曼光谱的信噪比。为了解决这一难题,科研人员开发出了不同方式的拉曼信号增强技术,以提高拉曼信号的强度。目前常用的拉曼信号增强技术主要有共振拉曼光谱技术(RRS)[16-20]、表面增强拉曼光谱技术(SERS)[21-27]、针尖增强拉曼光谱技术(TERS)[28-33]和受激拉曼光谱技术(SRS)[34-38]。这些技术都具有很高的生物化学灵敏度和选择性,并且无需对样品进行标记,在生物和医学领域有着广阔的应用前景。

拉曼光谱成像技术基于样品的拉曼光谱生成详细的化学图像,在该图像的每一个单元上,都对应采集了一条完整的拉曼光谱,将这些光谱集成在一起,就可生成一幅反映材料成分和结构的伪彩色图像[37-40]。拉曼光谱成像技术可以根据拉曼峰的强度生成不同构型的图像,如材料浓度和分布图像[41]、分子结构[42-43]、应力图像[44]、结晶度图像[45],

也可以与光纤探头组合进行原位组织成像[46-50]，其应用场景多种多样[51-54]。

3 基于拉曼光谱的肿瘤诊断

3.1 基于拉曼光谱的诊断方式

拉曼光谱技术是一种具有特异性、无需标记等优点的光学技术，研究人员可以通过拉曼峰频移的位置或拉曼峰强度等来分析物质的生化组成，从而对肿瘤组织的性质进行判断。传统的基于拉曼光谱的肿瘤诊断方法通常采集肿瘤组织或癌细胞系、血液或血液成分、肿瘤标志物等原材料进行拉曼光谱数据的采集。所采集的拉曼数据多为一维数据，且多采用主成分分析-线性判别分析（PCA-LDA）等多变量统计分析方法来分析光谱的细微差异，从而实现对不同肿瘤的诊断。目前，该方法已经能够诊断出身体不同部位的恶性肿瘤（癌症），如膀胱癌[55-58]、脑癌[59-61]、乳腺癌[62-72]、宫颈癌[73-76]、结直肠癌[77-79]、食管癌[68,80]、胃癌[81-84]、喉癌[85]、肝癌[86-89]、肺癌[90-98]、鼻咽癌[99-101]、口腔癌[24,74,80,102-104]、卵巢癌[105-108]、胰腺癌[109]、前列腺癌[110-115]、皮肤癌[116-119]、甲状腺癌[120-121]。尤其是肺癌，其作为癌症类型中新增病例和死亡病例最多的癌症类型[2]，一直都是研究的焦点；而乳腺癌，作为女性癌症类型中新发病例和死亡人数最多的癌种[2]，也受到了更多关注。

基于拉曼光谱的诊断方法通常是利用光谱仪从新鲜或储存的未加工样本中获取拉曼光谱，然后对光谱进行分析，以区分样本的类型与性质。对不同肿瘤组织的光谱进行采集和分类是拉曼光谱在诊断肿瘤性质方面最直接和最广泛的应用[57-59,61,69-73,75,85-87,97-98,104,108,110-112,116-120]。传统的术中组织学工作流程需要组织运输、标本处理、切片准备和诊断，所需时间为 30 min～1 h，甚至术前或术后的组织学诊断也需要 1～2 d，而基于拉曼光谱的肿瘤组织诊断方法则大大减少了诊断时间。

在检测尺度上，细胞比组织更精细，因此可以利用基于拉曼光谱的细胞检测对癌症进行筛查[79,96,120]。活细胞的拉曼光谱分析在高可靠性地区分细胞株后，可对疾病阶段进行分类，其作为一种细胞表型的诊断工具在临床上发挥着重要作用。实际上，对于研究人员来说，很难重复获得研究区域的组织切片，因此，脱落细胞学检查被认为是一种无创的方法，特别是可利用脱落细胞的拉曼光谱进行肿瘤的诊断与筛查[74,103]。

血液是一种重要的体液，其中包括血浆、红细胞、白细胞和血小板。血液中检测到的氧、营养素、废物和电解质水平通常被用于临床评估人类的健康。拉曼光谱技术是一种无标签的分析技术，被用于探测血液成分和全血已超过 40 年的历史，并已被证明是一种有用的应用技术[122]。当身体的某个器官发生癌变时，血液中的生化成分会随之发生变化。因此，研究人员就利用拉曼光谱来检测这些变化，用于癌症的诊断。利用血液或血液成分的拉曼光谱可以诊断的癌症有膀胱癌[55-56]、乳腺癌[62-65]、宫颈癌[76]、结直肠癌[77-78]、胃癌[82-84]、肝癌[88-89]、肺癌[90-92]、鼻咽癌[99-101]、口腔癌[102]、卵巢癌[105-106]、前列腺癌[114-115]、甲状腺癌[121]。由于全血成分复杂，仅有少数研究采用全血进行诊断[64,101]。血浆占血液总量的 50％以上，它是一种黄色的碱性水溶液，是由蛋白质、脂类、无机盐、糖、氨基酸、代谢废物和大量水组成的极其复杂的混合物。与细胞、组织等其他诊断样本相比，血浆样本更容易采集，更适合采用拉曼光谱技术进行快速、微创的癌症诊断[62-63,76-77,100,105-106,121]。血清是去除纤维蛋白原和凝血因子后从血浆中分离出来的淡黄色的透明液体。与血浆和血液相比，血清的成分较少，因此在拉曼光谱诊断肿瘤方面比血浆更受研究者的欢迎[55-56,65,78,82-84,88-92,99,102,114-115]。

对于研究者和病理学家来说，采用传统的活检技术重复获取肿瘤组织进行分析是很困难的。组织活检均有侵袭性，而且不适合用于早期诊断，只能捕捉肿瘤异质性的短期状况，通常无法实现疾病进化的精确时间监测[123-124]。肿瘤生物标记检测是一种非侵入性的快速分析技术，最近研究人员发现其具有解决传统活检局限性的潜力。肿瘤生物标志物包含肿瘤来源物质，如循环肿瘤细胞（CTCs）、循环核酸、蛋白质和外泌体等。这些物质的浓度低，化学成分复杂，拉曼光谱特别适合检测与分析这些物质。近年来，人们利用拉曼光谱技术对肿瘤生物标志物进行了多项研究，这些肿瘤生物标志物包括外泌体（如图 1(a)所示）[68,109]、腺嘌呤[80]、挥发性有机化合物（VOCs，如图 1(b)所示）[94]、胞外囊泡（EVs，如图 1(c)所示）[113]。

获取样品后，可以使用不同的拉曼仪器进行光谱采集。拉曼仪器可以采用不同波长的激发光，如波长为 532 nm[70,87,104]、633 nm[98,119]和 671 nm[110]的可见光，以及波长为 785 nm[57-59,69,71-73,85-86,110-111]、830 nm[116-118]和 1064 nm[71,97,112]的近红外光。可见
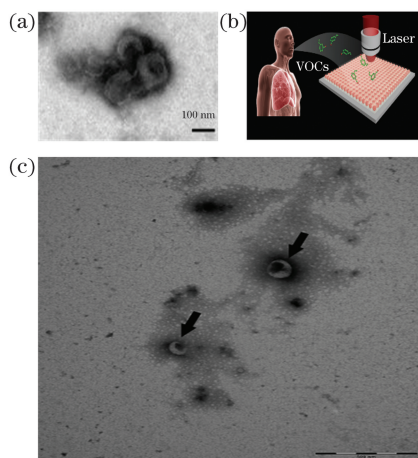
图 1 肿瘤生物标志物。(a)外泌体[68];(b)挥发性有机化合物[94];(c)胞外囊泡[113]

Fig. 1 Tumor markers. (a) Exosomes[68]; (b) volatile organic compounds[94]; (c) extracellular vesicles[113]

光的散射强度高于近红外,而近红外激发是为了减少组织的自发荧光。因此,应根据样品选择合适的激发光波长。

在拉曼光谱数据采集处理过程中,光谱的采集范围会影响采集时间和后续数据处理的冗余度。拉曼光谱的采集范围通常为 $400 \sim 3500$ cm^{-1},而该波数区通常可分为三部分,即拉曼指纹区(FP,$400 \sim 1800$ cm^{-1})、高波数区(HW,$2800 \sim 3200$ cm^{-1})和中间区,中间区通常没有拉曼特征峰。在全部的波数区间进行采集是非常耗时的,之后还需要从整个光谱中提取片段进行数据处理[57-59,69,108]。因此,大多数研究简单地选择 FP 区域[70,72-73,85-87,97,104,111-112,116-118]或同时选择 FP 和 HW 区域[71,98,110]进行光谱数据的采集。Chen 等[58]研究了激光功率与积分时间对诊断精度的影响,结果表明,增大激光功率对整体预测精度的影响不大,但增加积分时间却能显著提高预测精度。

数据处理对肿瘤分类至关重要。研究人员通常先利用各种算法对获得的光谱进行滤波、归一化和校正处理,然后再进行分类。拉曼峰强度比较是最直接的方法,但精度不高[108,119]。采用蚁群优化算法(ACO)寻找最佳拉曼特征的方法[69]以及基于欧氏距离和马氏距离的峰值强度进行判别分析的方法[117]可以提高诊断精度。但对于大量的数据,研究人员往往采用丰富的多元统计分析方法来分析光谱的差异。多元统计分析方法包括人工神经网络(ANN)[57]、PCA[59,73,116]、PCA-LDA[71-72,85-87,97-98,104]、偏最小二乘-判别分析(PLS-

DA)[75]、支持向量机(SVM)[110,112]等。Chen 等[58]和 Lyng 等[70]评估了不同算法对同一批样品的诊断效果;Garcia 等[118]提出了一种基于非经典逻辑的 PL(para-consistent logic)技术,与主成分分析方法相比,PL 技术的准确率更高。随着计算机科学和技术的发展,采用机器学习模型进行分类的方法被应用于组织诊断,该方法具有较高的灵敏度和特异性[111]。

表面增强拉曼光谱技术(SERS)是一种十分优异的拉曼增强技术,它可在保证光谱分辨率的情况下获得极高的信噪比,甚至能够实现单分子信号的捕捉[22]。SERS 技术的灵敏度和测量速度是传统拉曼技术不能比拟的。SERS 的原理为:当分子吸附在粗糙金属表面等纳米结构上时,局域电磁场等的增强作用可将拉曼光谱的信号强度提升 $10^{10} \sim 10^{11}$ 倍[125]。SERS 的关键在于如何制备增强基底或纳米增强材料,常用的纳米材料多为金材料,如金纳米结构(AuNFs,如图 2(a)所示)[126-129]、金纳米粒(AuNPs,如图 2(b)所示)[130-137]、金纳米棒(AuNRs)[138]、金纳米星(AuNSs,如图 2(c)所示)[139-141],也有人采用的纳米材料是银材料(如图 2(d)所示)[64,142-150]以及金银纳米粒(如图 2(e)所示)[151-154]。此外,科研人员还研究出了一些其他材料,如钛合金(如图 2(f)所示)[155]、TiO$_2$(如图 2(g)所示)[156]、CeO$_2$(如图 2(h)所示)[157]。由于 SERS 不仅大大增强了探测物质的拉曼信号,还会对 SERS 材料进行二次处理,如增加靶向体或者配体,因此在实际中对肿瘤进行诊断时,多利用肿瘤标志物来进行定量诊断,或直接利用拉曼信号的特征峰强度对比来诊断,从而极大地提高了肿瘤诊断的准确性。

综上所述,基于拉曼光谱的诊断方式的主要着力点在于寻找正常样本与癌变样本之间的拉曼特征峰差异,这种差异相对来说不是很明显,而且现有的拉曼光谱数据处理方法所能处理的样本数据量有限,对于大量或者海量数据来说,现有的数据处理方式在寻找拉曼峰的差异性方面存在一定不足。未来,一方面应加大对各种拉曼光谱增强技术的研究,使原有特征峰隐含的差异性显现出来;另一方面,应寻找更好的数据处理方法来对大量或海量样本进行数据处理,从而对肿瘤的癌变情况进行诊断。

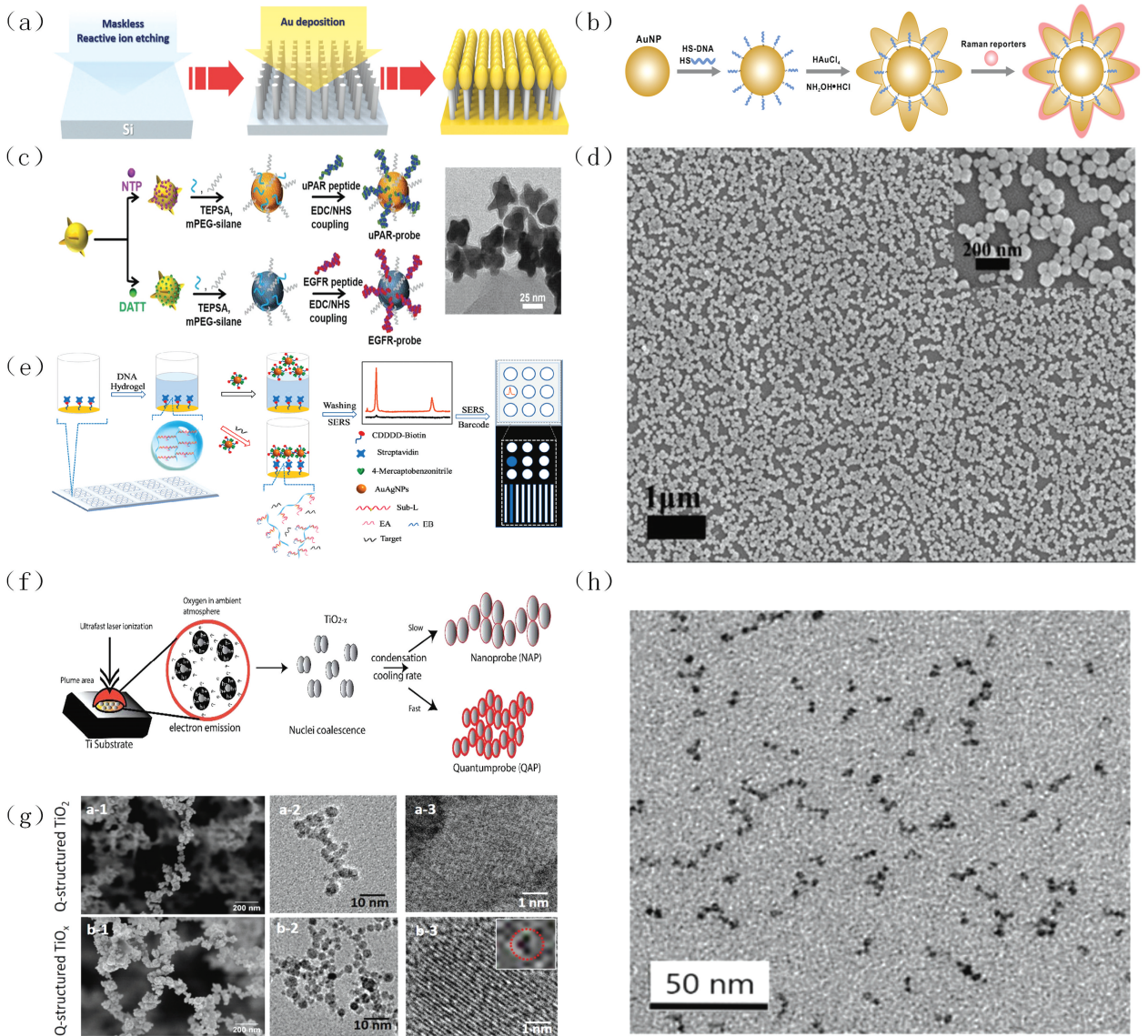### 3.2 基于拉曼成像的诊断方式

拉曼光谱成像技术通过对生物材料中的化学

图 2 SERS 材料。(a)金纳米结构[128];(b)金纳米粒[133];(c)金纳米星[139];(d)银纳米星[144];(e)金银纳米粒[151];(f)钛合金[155];(g)TiO₂[156];(h)CeO₂[157]

Fig. 2 SERS materials. (a) AuNFs[128]; (b) AuNPs[133]; (c) AuNSs[139]; (d) AgNPs[144]; (e) AuAgNPs[151]; (f) titanium alloy[155]; (g) TiO₂[156]; (h) CeO₂[157]

键进行无标记快速表征来实现非破坏性、实时的原位分析检测,已在肿瘤检测和诊断领域进行了初步尝试与应用。拉曼光谱成像技术在区分肿瘤组织细胞与正常细胞以及标准手术条件下无法检测到的肿瘤边缘等方面具有极大优势,同时,在肿瘤组织的亚型与分期的判断上具有很大的应用空间,然而其对于恶性肿瘤组织细胞检测的灵敏度与特异性还有待提高。机器学习等人工智能算法的引入[158-161],使得拉曼光谱成像技术在肿瘤组织细胞检测中的时效性及精确性明显提高。

相干拉曼散射(CRS)显微术是一种振动光谱成像技术,它不需要标记的高生化敏感性和选择性,在生物医学系统中有着广泛应用。常见的 CRS 有相干反斯托克斯拉曼散射(CARS)和受激拉曼散射(SRS)两种,它们在肿瘤诊断上已被广泛应用[161-169],如:利用 SRS 技术对脑瘤[161]、颅底肿瘤(如图 3(a)所示)[162]和结肠癌(如图 3(b)所示)[163]组织进行成像与诊断;利用 SRS 对正常和癌变肝组织的脂质代谢产物进行成像[164],如图 3(c)所示;利用 SRS 研究胰腺癌细胞在饥饿和化疗药物胁迫下的代谢反应[165];利用 CARS 实现人体宫颈癌细胞(HeLa cell)和口腔细胞(Buccal cell)的超分辨显微成像[167]。
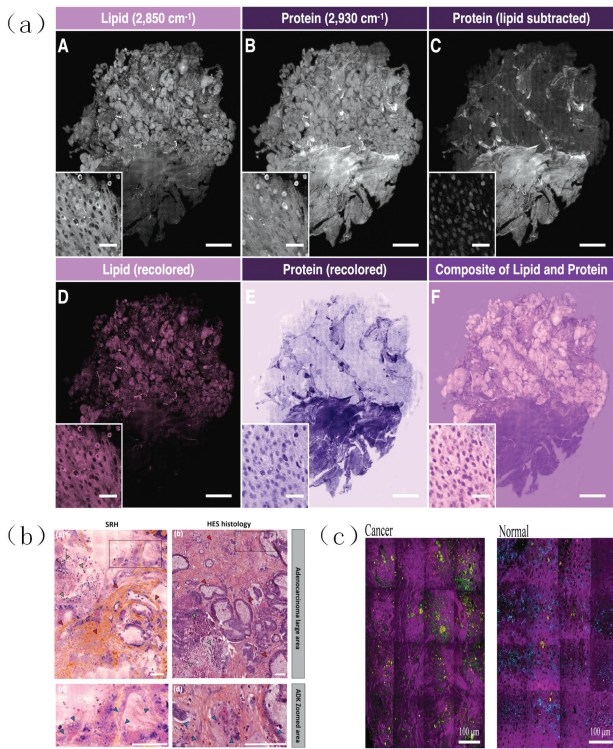
SERS 纳米探针以其指纹样光谱的高灵敏度和

图 3 相干拉曼散射成像。(a)脑膜瘤组织[162];(b)人结肠腺[163];(c)癌组织和邻近的正常肝组织[164]

Fig. 3 CRS Imaging. (a) Meningioma tissue[162]; (b) human colon adenocarcinoma[163]; (c) cancerous and adjacent normal liver tissues[164]

特异性,在肿瘤成像领域显示出巨大的潜力,已在膀胱癌组织[170]、肺癌 A549 细胞[171]、肝癌 HepG2 细胞[171]、宫颈癌 HeLa 细胞[172]、乳腺癌 BT-20 细胞[173]、乳腺癌 MCF-7 细胞[173-179]、乳腺癌 MDA-MB-231 细胞[179]、胃癌 MGC-803 细胞[177-178]成像等方面被广泛应用。此外,人们也研究了一些新型纳米增强材料,并在动物身上进行了验证,如将卵巢癌[180]、脑瘤[181]、乳腺癌[182]接种到小鼠身上进行 SERS 成像,为这些材料在各种肿瘤诊断的应用上打下了基础[180-185]。

共聚焦拉曼显微光谱仪(CRM)具有良好的空间分辨率,可以得到微小体积和样品不同深度处的光谱信息,还能消除物镜自身带来的光谱,因此利用 CRM 对肿瘤进行成像诊断具有很大的应用空间[186-192],如:利用共聚焦拉曼显微光谱成像(CRMI)研究肺鳞状细胞癌对微波消融治疗的复杂生化反应[186];探究不同激发光生成的人体非癌和癌性结肠组织样本的拉曼光谱和成像的区别[188];利用 CRMI 探索的拉曼生物标志物指导基底细胞癌边缘的切除[190-191];利用 CRMI 检测人类乳房、小

肠、脑肿瘤组织以及正常的人星形胶质细胞和原发胶质母细胞瘤 U-87 MG 细胞系中磷酸化蛋白的光谱变化,以探究细胞内致癌代谢途径[192]。

对于目前使用机器学习进行的智能化诊断来说,拉曼成像所形成的伪色彩图片是非常合适的输入样本,这也是未来应用拉曼成像方式进行肿瘤诊断的重要途径。应用拉曼成像方式进行人工智能化识别,首先要解决的是拉曼成像图像与现有切片病理诊断图像的一致性,只有在两者具有高度一致的情况下,才能为下一步的智能识别打下坚实的基础。Zhang 等[160]探究了喉癌组织与正常组织的苏木精-伊红(H&E)染色图像与拉曼成像图像的一致性,如图 4 所示,结果表明两者具有 90% 以上的诊断一致性。在标准组织学图像与拉曼成像图像高度一致的情况下,将这些图像作为深度学习的输入样本,采用不同的机器学习方法(如深度卷积神经网络[158-159]、残差卷积神经网络[160]和决策树机器学习模型[161]),可以实现基于拉曼成像方式的肿瘤诊断。Hollon 等[158]设计了结合受激拉曼组织学(SRH)与深度神经网络的诊断流程,该诊断流程实现了术中 150 s 内得到脑瘤的诊断结果,远少于术中组织学耗时(20~30 min)。

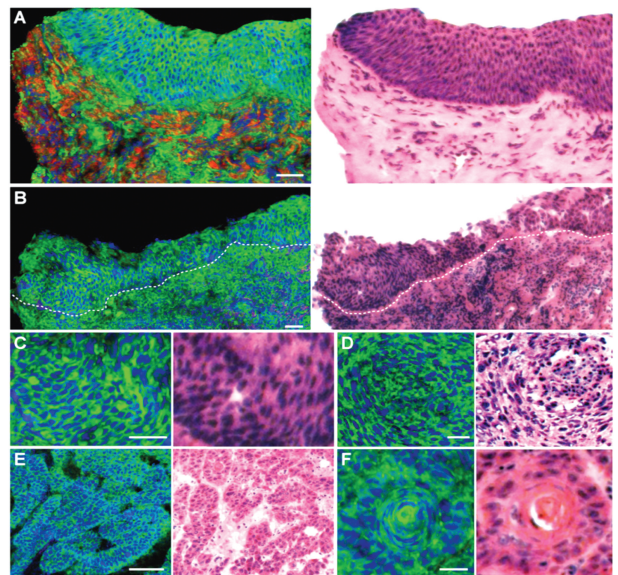综上所述,基于拉曼成像的诊断方式的关键在于寻找正常样本与癌变样本成像的差异性。图像之间的差异性比拉曼特征峰之间的差异性更加明显,而且图像是可以根据形态学进行诊断的,从而

图 4 喉鳞状细胞癌组织冰冻切片的 SRS 和 H&E 图像[160]
Fig. 4 SRS and H&E images of frozen sections from laryngeal squamous cell carcinoma tissues[160]

使得诊断更加精确。未来,应发展更为精细的拉曼成像技术,提高成像分辨率,同时可将机器学习等人工智能模式引入到成像诊断过程中,提高诊断的客观性、准确性与实时性。拉曼成像结合人工智能是未来拉曼成像诊断的重中之重。

3.3 探头结合光谱的诊断方式

随着光学技术的发展,光纤技术与信号传输系统的结合使得部分肿瘤的诊断可以由光纤将拉曼信号加载并传播出来,从而对肿瘤进行诊断[57,111,193-205]。光纤与内镜联用,或者用光纤探头进行肿瘤诊断,是未来应用拉曼光谱技术进行原位实时肿瘤诊断的一个重要研究方向,也是一种新型快速的肿瘤诊断方法。

使用光纤探头进行拉曼光谱数据的采集或者成像是一种较为方便的拉曼光谱诊断方法,该方法主要被应用于体外组织切片的诊断,具有操作简单、安全性高等特性,目前已被应用于多种癌症的诊断,如利用手持式光纤探头对膀胱癌[57,193]、前列腺癌[111]、结直肠癌[194]、脑癌[195-196]、乳腺癌[197]、食管癌[198]、皮肤癌[199]进行组织光谱的采集或成像。

相比于体外诊断,利用光纤探头进行体内肿瘤诊断的难度更大,安全性更差,但也有一些科研成果的产出。如:Desroches 等[200]设计了一种新型穿刺针,如图5(a)所示,它既能获取活检组织样品,又能对穿刺部分进行拉曼光谱采集,从而快速地对脑部活检位置进行诊断;Han 等[201]开发了一种表面增强共振拉曼散射(SERRS)探头,并在该探头的辅助下,对背侧皮肤腔中预先进行胶质瘤异种移植的小鼠实施了脑肿瘤的逐步切除,直至切除部位的探针拉曼信号完全消失,如图5(b)所示。Shams 等[202]开发了一种用于空间跟踪拉曼光谱探针的原位成像导航系统,该系统采用结直肠超声/磁共振(TRUS/MR)成像引导,并用模拟组织和体外前列腺进行了测试,该系统在前列腺癌患者的离体前列腺测试中对高级别病变的检测准确率达到了81%。McGregor 等[203]研发了一种新型微型拉曼探针,如图5(c)所示,该探针可以捕捉到肺周围的结构,并且成功获得了活体正常组织和癌结节肺周围的拉曼光谱。该探针收集到的光谱显示了脂质、蛋白和脱氧血红蛋白的特征,有助于进一步的病理分类。

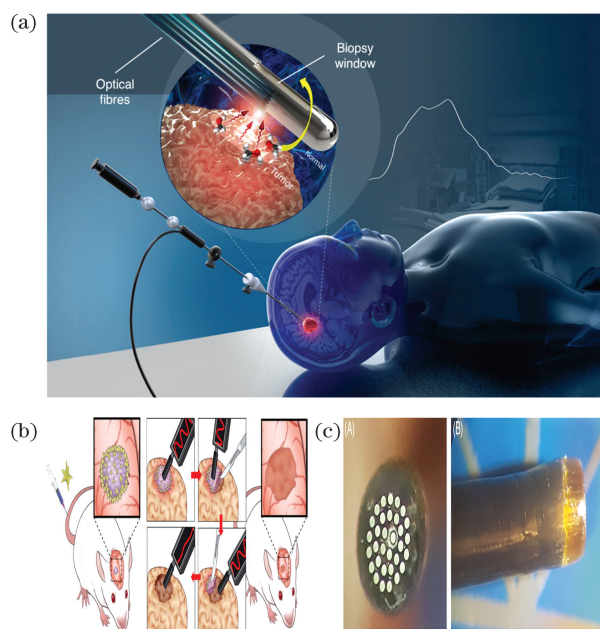光纤与内镜系统的联用是一种新型的用于肿瘤体内诊断的方法,其优势在于不仅可以获得肿瘤的实时成像,还可以同时进行拉曼光谱数据采集或拉曼成像。Bergholt 等[48]开发了一种光纤拉曼内

图 5 体内成像。(a)光学芯针活检示意图[200];(b)SERRS引导下的胶质瘤手术[201];(c)拉曼探针[203]

Fig. 5 *In vivo* imaging. (a) Schematic representation of the optical core needle biopsy[200]; (b) procedure of SERRS-guided glioma surgery[201]; (c) Raman probe[203]

镜系统,如图6(a)所示,利用该系统可以从结肠组织表面以下同时获取指纹图谱和高波数拉曼光谱,用于实时评估结直肠癌变。Garai 等[49]研发了一种将微型非接触式光机电拉曼装置作为附件的临床内镜,如图6(b)所示,利用生物标志物靶向的表面增强拉曼散射纳米颗粒,实现了对空腔器官(如结肠和食管)腔表面的周向扫描。Wang 等[50]基于表面增强拉曼散射纳米颗粒,局部应用微型光谱内镜成像系统对食管腔内进行了综合成像,如图6(c)所示,结果发现,肿瘤定位可视化和生物标志物表达的定量与免疫组织化学和流式细胞术验证数据一致。Lin 等[204]结合白光成像、自发荧光成像、漫反射光谱和拉曼光谱技术,开发了一套完整的四模态内镜系统,并将其用于体内内镜下肿瘤的检测,如图6(d)所示。

综上所述,光纤与内镜联用或者用光纤探头直接进行肿瘤诊断的优势是方便快捷,尤其是针对体内诊断。未来,探头结合光谱的诊断方式在体内诊断、原位诊断等方面有着广阔的应用空间。特别地,将实时成像系统与机器学习识别模型相结合,将会大大提高诊断的时效性,实现近实时智能诊断。
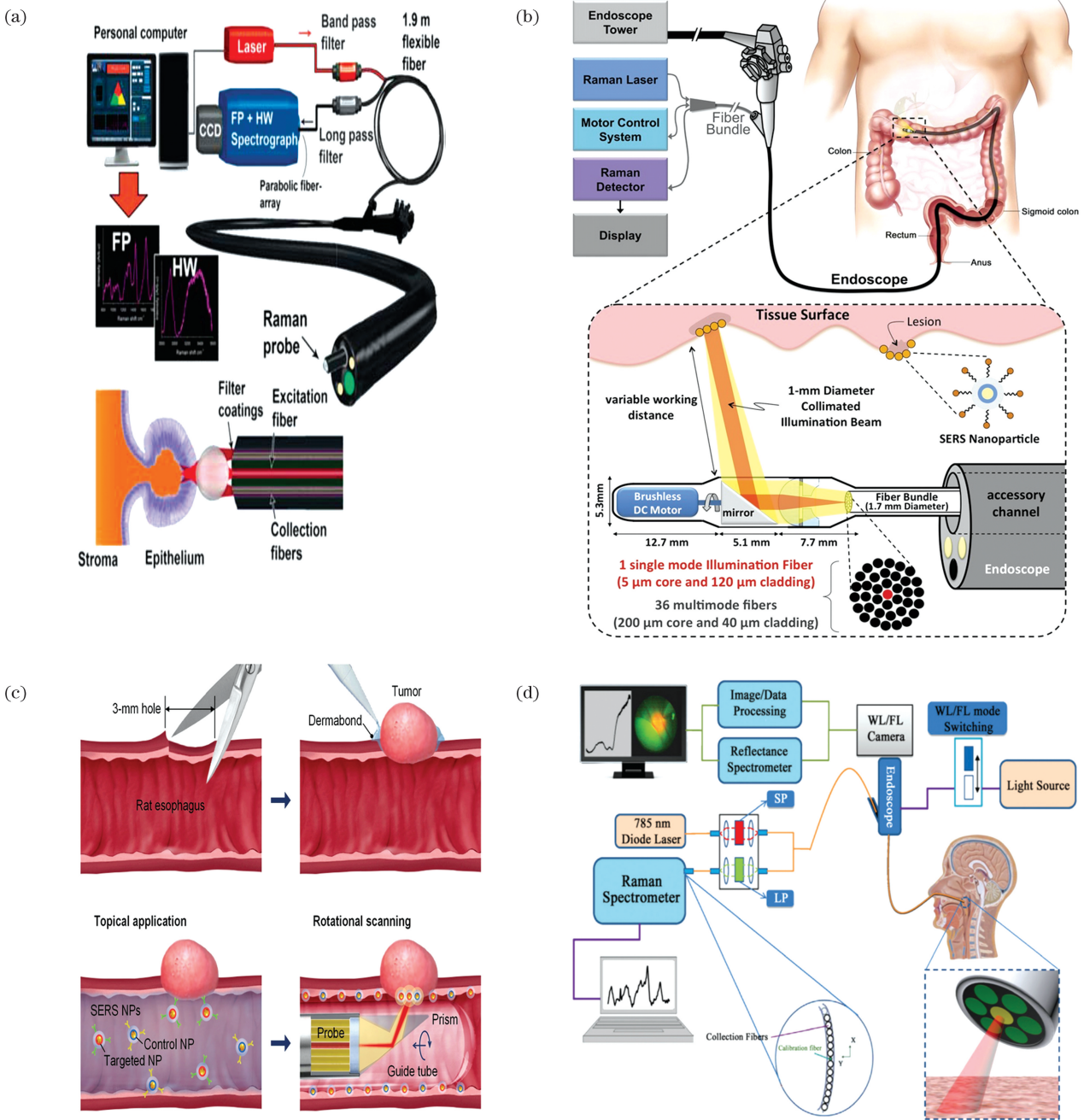
图 6 光纤与内镜系统成像。(a)结肠镜检查的拉曼光谱系统[48];(b)与白光内镜并行使用的拉曼成像系统原理图[49];
(c)大鼠食管肿瘤模型的建立和内镜成像示意图[50];(d)综合内镜成像和光谱系统的原理图[204]

Fig. 6 Optical fiber and endoscope system imaging. (a) Raman spectroscopy system at colonoscopy[48]; (b) schematic of Raman-imaging system being used in parallel with white-light endoscopy[49]; (c) schematic of establishment and endoscopic imaging of a rat esophageal tumor model[50]; (d) schematic of integrated endoscopic imaging and spectroscopy system[204]

4 结束语

国内外科研人员一直都在寻找肿瘤的诊断与治疗方法,并取得了一些重大进展,然而目前很多恶性肿瘤的发病机理仍不清晰,治疗方法也比较单

一。面对肿瘤,科研人员与医生还是处于"后发制瘤"的阶段。因此,如何能够尽早地发现肿瘤,并进行诊断与治疗,对人类的生命健康尤为重要。

鉴于目前肿瘤的检测手段存在诊断时间长、创伤严重、误判率高、严重依赖于医生的主观经验等

问题,亟需开发出具有智能属性的肿瘤诊断技术。拉曼光谱技术作为一种无损、无需标记的光学技术,可以通过拉曼峰频移的位置来分析物质的生化组成,在肿瘤的良恶性判别上越来越受到科研人员的青睐。然而,大多数基于拉曼光谱的诊断方式,仅仅是对拉曼光谱进行数据处理,而且拉曼谱图中包含的肿瘤信息相对较少,因此,这种方法多用于肿瘤良恶性的诊断。该诊断方式在实际中实施时,相对来说获取样品方便快捷,数据处理方法简单易行,诊断结果可以快速给出,且诊断结果具有较高的准确性。但是对于患者肿瘤的精准诊断来说,仅仅检测出肿瘤的良恶性还是远远不够的,因此需要科研人员更加深入地探究如何运用拉曼光谱技术对肿瘤的类型与亚型进行诊断。拉曼光谱成像技术是一种能提供多种信息的光谱技术,例如形态学信息,从而使得这种方式更适合用于对肿瘤进行进一步的分类分型诊断。然而,这种方式获取的样品信息较为复杂,且所需时间较长。随着计算机科学的发展,应用深度学习算法对肿瘤的拉曼成像进行分类分型诊断是大幅提高肿瘤诊断准确率的关键。但是,拉曼成像结果与现有免疫组化成像结果的一致性仍需要进一步提高。随着光学技术的发展,光纤技术与内镜系统的结合,使得部分肿瘤的诊断可以由光纤将拉曼信号加载并传播出来,从而对肿瘤进行诊断。光纤与内镜联用或者用手持光纤探头进行肿瘤诊断,是未来应用拉曼光谱进行原位实时肿瘤诊断的一个重要方向,也是一种新型、快速的肿瘤诊断方法。此外,深度学习等计算机科学技术为肿瘤的拉曼成像分析提供了一种具有智能属性的肿瘤诊断方法,是未来肿瘤诊断的一个全新的科学途径,甚至可以替代病理科医生进行诊断,这将会极大地促进肿瘤诊断医学的发展。

总而言之,基于拉曼光谱技术的肿瘤诊断方法具有广阔的应用前景,可为现有的肿瘤诊断方法提供有效的补充,甚至在不远的将来,有望替代现有的诊断方法。

参 考 文 献

[1] Cao M M, Chen W Q. Epidemiology of cancer in China and the current status of prevention and control [J]. Chinese Journal of Clinical Oncology, 2019, 46 (3): 145-149.
曹毛毛, 陈万青. 中国恶性肿瘤流行情况及防控现状 [J]. 中国肿瘤临床, 2019, 46(3): 145-149.

[2] Bray F, Ferlay J, Soerjomataram I, et al. Global cancer statistics 2018: GLOBOCAN estimates of incidence and mortality worldwide for 36 cancers in 185 countries[J]. CA, 2018, 68(6): 394-424.

[3] Chen W Q, Zheng R S, Baade P D, et al. Cancer statistics in China, 2015[J]. CA, 2016, 66(2): 115-132.

[4] Huang Q, Ouyang X N. Predictive biochemical-markers for the development of brain metastases from lung cancer: clinical evidence and future directions[J]. Cancer Epidemiology, 2013, 37(5): 703-707.

[5] Inamura K, Ishikawa Y. MicroRNA in lung cancer: novel biomarkers and potential tools for treatment [J]. Journal of Clinical Medicine, 2016, 5(3): 36.

[6] Rice S L, Friedman K P. Clinical PET-MR imaging in breast cancer and lung cancer[J]. PET Clinics, 2016, 11(4): 387-402.

[7] Rebouças Filho P P, Cortez P C, da Silva Barros A C, et al. Novel and powerful 3D adaptive crisp active contour method applied in the segmentation of CT lung images[J]. Medical Image Analysis, 2017, 35: 503-516.

[8] Vansteenkiste J, Fischer B M, Dooms C, et al. Positron-emission tomography in prognostic and therapeutic assessment of lung cancer: systematic review[J]. The Lancet Oncology, 2004, 5(9): 531-540.

[9] Lian C F, Ruan S, Denoeux T, et al. Selecting radiomic features from FDG-PET images for cancer treatment outcome prediction [J]. Medical Image Analysis, 2016, 32: 257-268.

[10] Gal A A. In search of the origins of modern surgical pathology [J]. Advances in Anatomic Pathology, 2001, 8(1): 1-13.

[11] Gutmann E J. Pathologists and patients: can we talk?[J]. Modern Pathology, 2003, 16(5): 515-518.

[12] Lechago J. The frozen section: pathology in the trenches[J]. Archives of Pathology & Laboratory Medicine, 2005, 129(12): 1529-1531.

[13] Raman C V, Krishnan K S. A new type of secondary radiation[J]. Nature, 1928, 121(3048): 501-502.

[14] Kneipp K, Kneipp H, Itzkan I, et al. Ultrasensitive chemical analysis by Raman spectroscopy [J]. Chemical Reviews, 1999, 99(10): 2957-2975.

[15] Movasaghi Z, Rehman S, Rehman I U. Raman spectroscopy of biological tissues [J]. Applied Spectroscopy Reviews, 2007, 42(5): 493-541.

[16] Zhao L F, Mu X J. Visualization of vibrational-resolution charge transfer enhanced resonance Raman scattering spectroscopy[J]. Spectrochimica Acta Part A, 2020, 229: 117945.

[17] Wade J, Pugh H, Nightingale J, et al. Colour in bivalve shells: using resonance Raman spectroscopy to compare pigments at different phylogenetic levels [J]. Journal of Raman Spectroscopy, 2019, 50(10): 1527-1536.

[18] Liu S L, Ma H, Zhu J Y, et al. Ferrous cytochrome c-nitric oxide oxidation for quantification of protein S-nitrosylation probed by resonance Raman spectroscopy[J]. Sensors and Actuators B, 2020, 308: 127706.

[19] Buhrke D, Hildebrandt P. Probing structure and reaction dynamics of proteins using time-resolved resonance Raman spectroscopy [J]. Chemical Reviews, 2020, 120(7): 3577-3630.

[20] Browne W R. Resonance Raman spectroscopy and its application in bioinorganic chemistry[M]//Practical approaches to biological inorganic chemistry. Amsterdam: Elsevier, 2020: 275-324.

[21] Jeanmaire D L, Vanduyne R P. Surface Raman spectroelectrochemistry Part 1. Heterocyclic, aromatic, and aliphatic-amines adsorbed on anodized silver electrode [J]. Journal of Electroanalytical Chemistry, 1977, 84(1): 1-20.

[22] le Ru E C, Meyer M, Etchegoin P G. Proof of single-molecule sensitivity in surface enhanced Raman scattering (SERS) by means of a two-analyte technique[J]. The Journal of Physical Chemistry B, 2006, 110(4): 1944-1948.

[23] Li Z F, Li C, Lin D, et al. Surface-enhanced Raman spectroscopy for differentiation between benign and malignant thyroid tissues[J]. Laser Physics Letters, 2014, 11(4): 045602.

[24] Fălămaș A, Rotaru H, Hedeșiu M. Surface-enhanced Raman spectroscopy (SERS) investigations of saliva for oral cancer diagnosis [J]. Lasers in Medical Science, 2020, 35(6): 1393-1401.

[25] Cialla-May D, Zheng X, Weber K, et al. Recent progress in surface-enhanced Raman spectroscopy for biological and biomedical applications: from cells to clinics[J]. Chemical Society Reviews, 2017, 46(13): 3945-3961.

[26] Talley C E, Jusinski L, Hollars C W, et al. Intracellular pH sensors based on surface-enhanced Raman scattering[J]. Analytical Chemistry, 2004, 76(23): 7064-7068.

[27] Ru E C L, Blackie E, Meyer M, et al. Surface enhanced Raman scattering enhancement factors: a comprehensive study [J]. Journal of Physical Chemistry C, 2007, 111(37): 13794-13803.

[28] Wang X, Huang S C, Huang T X, et al. Tip-enhanced Raman spectroscopy for surfaces and interfaces[J]. Chemical Society Reviews, 2017, 46 (13): 4020-4041.

[29] Sonntag M D, Pozzi E A, Jiang N, et al. Recent advances in tip-enhanced Raman spectroscopy [J]. The Journal of Physical Chemistry Letters, 2014, 5 (18): 3125-3130.

[30] Zhang R, Zhang Y, Dong Z C, et al. Chemical mapping of a single molecule by plasmon-enhanced Raman scattering[J]. Nature, 2013, 498(7452): 82-86.

[31] Chen C, Hayazawa N, Kawata S. A 1.7 nm resolution chemical analysis of carbon nanotubes by tip-enhanced Raman imaging in the ambient [J]. Nature Communications, 2014, 5(1): 3312.

[32] Kumar N, Weckhuysen B M, Wain A J, et al. Nanoscale chemical imaging using tip-enhanced Raman spectroscopy[J]. Nature Protocols, 2019, 14 (4): 1169-1193.

[33] Chen X, Liu P, Hu Z, et al. High-resolution tip-enhanced Raman scattering probes sub-molecular density changes[J]. Nature Communications, 2019, 10(1): 2567.

[34] Zong C, Premasiri R, Lin H, et al. Plasmon-enhanced stimulated Raman scattering microscopy with single-molecule detection sensitivity[J]. Nature Communications, 2019, 10(1): 5318.

[35] Mittal R, Balu M, Krasieva T, et al. Evaluation of stimulated Raman scattering microscopy for identifying squamous cell carcinoma in human skin [J]. Lasers in Surgery and Medicine, 2013, 45(8): 496-502.

[36] Prince R C, Frontiera R R, Potma E O. Stimulated Raman scattering: from bulk to nano[J]. Chemical Reviews, 2017, 117(7): 5070-5094.

[37] Yang W, Li A, Suo Y, et al. Simultaneous two-color stimulated Raman scattering microscopy by adding a fiber amplifier to a 2 ps OPO-based SRS microscope [J]. Optics Letters, 2017, 42(3): 523-526.

[38] Ozeki Y, Kitagawa Y, Sumimura K, et al. Stimulated Raman scattering microscope with shot noise limited sensitivity using subharmonically

synchronized laser pulses[J]. Optics Express, 2010, 18(13): 13708-13719.

[39] Ranjan R, Indolfi M, Ferrara M A, et al. Implementation of a nonlinear microscope based on stimulated Raman scattering [J]. Journal of Visualized Experiments, 2019(149): e59614.

[40] Krafft C, Schie I W, Meyer T, et al. Developments in spontaneous and coherent Raman scattering microscopic imaging for biomedical applications[J]. Chemical Society Reviews, 2016, 45(7): 1819-1849.

[41] Gawinkowski S, Pszona M, Gorski A, et al. Single molecule Raman spectra of porphycene isotopologues [J]. Nanoscale, 2016, 8(6): 3337-3349.

[42] Liu P C, Chen X, Ye H P, et al. Resolving molecular structures with high-resolution tip-enhanced Raman scattering images[J]. ACS Nano, 2019, 13(8): 9342-9351.

[43] Laptenok S P, Rajamanickam V P, Genchi L C, et al. Fingerprint-to-CH stretch continuously tunable high spectral resolution stimulated Raman scattering microscope[J]. Journal of Biophotonics, 2019, 12 (9): e201900028.

[44] Batten T, Milikofu O. Characterising strain/stress and defects in SiC wafers using Raman imaging[J]. Materials Science Forum, 2015, 821/822/823: 229-232.

[45] Motoyama M, Ando M, Sasaki K, et al. Simultaneous imaging of fat crystallinity and crystal polymorphic types by Raman microspectroscopy[J]. Food Chemistry, 2016, 196: 411-417.

[46] Wood J J, Kendall C, Hutchings J, et al. Evaluation of a confocal Raman probe for pathological diagnosis during colonoscopy[J]. Colorectal Disease, 2014, 16 (9): 732-738.

[47] Jermyn M, Mok K, Mercier J, et al. Intraoperative brain cancer detection with Raman spectroscopy in humans[J]. Science Translational Medicine, 2015, 7 (274): 274ra19.

[48] Bergholt M S, Lin K, Wang J F, et al. Simultaneous fingerprint and high-wavenumber fiber-optic Raman spectroscopy enhances real-time in vivo diagnosis of adenomatous polyps during colonoscopy[J]. Journal of Biophotonics, 2016, 9(4): 333-342.

[49] Garai E, Sensarn S, Zavaleta C L, et al. A real-time clinical endoscopic system for intraluminal, multiplexed imaging of surface-enhanced Raman scattering nanoparticles[J]. PLoS One, 2015, 10 (4): e0123185.

[50] Wang Y W, Kang S, Khan A, et al. In vivo multiplexed molecular imaging of esophageal cancer via spectral endoscopy of topically applied SERS nanoparticles[J]. Biomedical Optics Express, 2015, 6(10): 3714-3723.

[51] Tiberj A, Camara N, Godignon P, et al. Micro-Raman and micro-transmission imaging of epitaxial graphene grown on the Si and C faces of 6H-SiC[J]. Nanoscale Research Letters, 2011, 6(1): 478.

[52] Suda J, Suwa S, Mizuno S, et al. Micro-Raman imaging on 4H-SiC in contact with the electrode at room temperature[J]. Spectrochimica Acta Part A, 2018, 193: 393-396.

[53] Wu J P. Linear quantification calibration of crystallinity at subpercent and its evaluation based on spectral and spatial information inherited in Raman chemical images[J]. Journal of Raman Spectroscopy, 2014, 45(8): 686-695.

[54] Wang P, Anderson E J D, Muller E A, et al. Hyper-spectral Raman imaging correlating chemical substitution and crystallinity in biogenic hydroxyapatite: dentin and enamel in normal and hypoplastic human teeth [J]. Journal of Raman Spectroscopy, 2018, 49(9): 1559-1567.

[55] Zhang Y J, Lai X P, Zeng Q Y, et al. Classifying low-grade and high-grade bladder cancer using label-free serum surface-enhanced Raman spectroscopy and support vector machine[J]. Laser Physics, 2018, 28 (3): 035603.

[56] Chen S, Zhu S S, Cui X Y, et al. Identifying non-muscle-invasive and muscle-invasive bladder cancer based on blood serum surface-enhanced Raman spectroscopy[J]. Biomedical Optics Express, 2019, 10(7): 3533-3544.

[57] Chen H, Li X, Broderick N, et al. Identification and characterization of bladder cancer by low-resolution fiber-optic Raman spectroscopy [J]. Journal of Biophotonics, 2018, 11(9): e201800016.

[58] Chen H, Li X, Broderick N G R, et al. Low-resolution fiber-optic Raman spectroscopy for bladder cancer diagnosis: a comparison study of varying laser power, integration time, and classification methods [J]. Journal of Raman Spectroscopy, 2020, 51(2): 323-334.

[59] Galli R, Meinhardt M, Koch E, et al. Rapid label-free analysis of brain tumor biopsies by near infrared Raman and fluorescence spectroscopy: a study of 209 patients[J]. Frontiers in Oncology, 2019, 9: 1165.

[60] Kowalska A A, Berus S, Szleszkowski Ł, et al. Brain tumour homogenates analysed by surface-enhanced Raman spectroscopy: discrimination among healthy and cancer cells[J]. Spectrochimica Acta Part A: Molecular and Biomolecular Spectroscopy, 2020, 231: 117769.

[61] Lemoine E, Dallaire F, Yadav R, et al. Feature engineering applied to intraoperative *in vivo* Raman spectroscopy sheds light on molecular processes in brain cancer: a retrospective study of 65 patients[J]. Analyst, 2019, 144(22): 6517-6532.

[62] Krishnamoorthy C, Prakasarao A, Srinivasan V, et al. Monitoring of breast cancer patients under pre and post treated conditions using Raman spectroscopic analysis of blood plasma [J]. Vibrational Spectroscopy, 2019, 105: 102982.

[63] Nargis H F, Nawaz H, Ditta A, et al. Raman spectroscopy of blood plasma samples from breast cancer patients at different stages[J]. Spectrochimica Acta Part A: Molecular and Biomolecular Spectroscopy, 2019, 222: 117210.

[64] Lin D, Wang Y Y, Wang T Y, et al. Metabolite profiling of human blood by surface-enhanced Raman spectroscopy for surgery assessment and tumor screening in breast cancer [J]. Analytical and Bioanalytical Chemistry, 2020, 412(7): 1611-1618.

[65] González-Solís J L. Discrimination of different cancer types clustering Raman spectra by a super paramagnetic stochastic network approach[J]. PLoS One, 2019, 14(3): e0213621.

[66] Zhang C, Winnard P T, Dasari S, et al. Label-free Raman spectroscopy provides early determination and precise localization of breast cancer-colonized bone alterations [J]. Chemical Science, 2018, 9 (3): 743-753.

[67] Moisoiu V, Socaciu A, Stefancu A, et al. Breast cancer diagnosis by surface-enhanced Raman scattering (SERS) of urine[J]. Applied Sciences, 2019, 9(4): 806.

[68] Zhang P, Wang L M, Fang Y P, et al. Label-free exosomal detection and classification in rapid discriminating different cancer types based on specific Raman phenotypes and multivariate statistical analysis[J]. Molecules, 2019, 24(16): 2947.

[69] Fallahzadeh O, Dehghani-Bidgoli Z, Assarian M. Raman spectral feature selection using ant colony optimization for breast cancer diagnosis[J]. Lasers in Medical Science, 2018, 33(8): 1799-1806.

[70] Lyng F M, Traynor D, Nguyen T N Q, et al. Discrimination of breast cancer from benign tumours using Raman spectroscopy[J]. PLoS One, 2019, 14 (2): e0212376.

[71] Zúñiga W C, Jones V, Anderson S M, et al. Raman spectroscopy for rapid evaluation of surgical margins during breast cancer lumpectomy [J]. Scientific Reports, 2019, 9(1): 14639.

[72] Vanna R, Morasso C, Marcinnò B, et al. Raman spectroscopy reveals that biochemical composition of breast microcalcifications correlates with histopathologic features[J]. Cancer Research, 2020, 80(8): 1762-1772.

[73] Woolford L, Chen M Z, Dholakia K, et al. Towards automated cancer screening: label-free classification of fixed cell samples using wavelength modulated Raman spectroscopy [J]. Journal of Biophotonics, 2018, 11(4): e201700244.

[74] Hole A, Tyagi G, Sahu A, et al. Exploration of Raman exfoliated cytology for oral and cervical cancers [J]. Vibrational Spectroscopy, 2018, 98: 35-40.

[75] Traynor D, Duraipandian S, Bhatia R, et al. The potential of biobanked liquid based cytology samples for cervical cancer screening using Raman spectroscopy[J]. Journal of Biophotonics, 2019, 12 (7): e201800377.

[76] Raja P, Aruna P, Koteeswaran D, et al. Characterization of blood plasma of normal and cervical cancer patients using NIR Raman spectroscopy [J]. Vibrational Spectroscopy, 2019, 102: 1-7.

[77] Li X Z, Yang T Y, Li C S, et al. Surface enhanced Raman spectroscopy (SERS) for the multiplex detection of BRAF, KRAS, and PIK3CA mutations in plasma of colorectal cancer patients [J]. Theranostics, 2018, 8(6): 1678-1689.

[78] Jenkins C A, Jenkins R A, Pryse M M, et al. A high-throughput serum Raman spectroscopy platform and methodology for colorectal cancer diagnostics[J]. Analyst, 2018, 143(24): 6014-6024.

[79] Gala de Pablo J, Armistead F J, Peyman S A, et al. Biochemical fingerprint of colorectal cancer cell lines using label-free live single-cell Raman spectroscopy [J]. Journal of Raman Spectroscopy, 2018, 49(8): 1323-1332.

[80] Dai W Y, Lee S, Hsu Y C. Discrimination between oral cancer and healthy cells based on the adenine

signature detected by using Raman spectroscopy[J].
Journal of Raman Spectroscopy, 2018, 49 (2):
336-342.

[81] Chen Y S, Cheng S L, Zhang A, et al. Salivary
analysis based on surface enhanced Raman scattering
sensors distinguishes early and advanced gastric
cancer patients from healthy persons[J]. Journal of
Biomedical Nanotechnology, 2018, 14(10): 1773-
1784.

[82] Bahreini M, Hosseinzadegan A, Rashidi A, et al. A
Raman-based serum constituents' analysis for gastric
cancer diagnosis: *in vitro* study[J]. Talanta, 2019,
204: 826-832.

[83] Guo L, Li Y P, Huang F R, et al. Identification and
analysis of serum samples by surface-enhanced
Raman spectroscopy combined with characteristic
ratio method and PCA for gastric cancer detection
[J]. Journal of Innovative Optical Health Sciences,
2019, 12(2): 1950003.

[84] Avram L, Iancu S D, Stefancu A, et al. SERS-based
liquid biopsy of gastrointestinal tumors using a
portable Raman device operating in a clinical
environment[J]. Journal of Clinical Medicine, 2020,
9(1): 212.

[85] Lai H C, Wan Z D, Wu Q, et al. Surface-enhanced
Raman spectroscopy for classification of laryngeal
cancer and adjacent tissues[J]. Laser Physics, 2019,
29(10): 105601.

[86] Lin K C, Xu J S, Li L, et al. Label-free detection of
liver cancer based on silver nanoparticles coated tissue
surface-enhanced Raman spectroscopy [J]. Laser
Physics Letters, 2018, 15(12): 125601.

[87] Zhang K, Hao C Y, Man B Y, et al. Diagnosis of
liver cancer based on tissue slice surface enhanced
Raman spectroscopy and multivariate analysis [J].
Vibrational Spectroscopy, 2018, 98: 82-87.

[88] Yu Y, Lin Y T, Xu C X, et al. Label-free detection
of nasopharyngeal and liver cancer using surface-
enhanced Raman spectroscopy and partial lease
squares combined with support vector machine[J].
Biomedical Optics Express, 2018, 9 (12): 6053-
6066.

[89] Zhu W F, Cheng L X, Li M, et al. Frequency shift
Raman-based sensing of serum MicroRNAs for early
diagnosis and discrimination of primary liver cancers
[J]. Analytical Chemistry, 2018, 90(17): 10144-
10151.

[90] Cao X W, Wang Z Y, Bi L Y, et al. Label-free

detection of human serum using surface-enhanced
Raman spectroscopy based on highly branched gold
nanoparticle substrates for discrimination of non-
small cell lung cancer [J]. Journal of Chemistry,
2018, 2018: 1-13.

[91] Wang H, Zhang S H, Wan L M, et al. Screening
and staging for non-small cell lung cancer by serum
laser Raman spectroscopy[J]. Spectrochimica Acta
Part A: Molecular and Biomolecular Spectroscopy,
2018, 201: 34-38.

[92] Wolny-Rokicka E, Tukiendorf A, Wydmański J, et
al. The potential of the quick detection of selectins
using Raman spectroscopy to discriminate lung cancer
patients from healthy subjects [J]. Journal of
Spectroscopy, 2018, 2018: 7843208.

[93] Qian K, Wang Y, Hua L, et al. New method of lung
cancer detection by saliva test using surface-enhanced
Raman spectroscopy[J]. Thoracic Cancer, 2018, 9
(11): 1556-1561.

[94] Qiao X Z, Su B S, Liu C, et al. Selective surface
enhanced Raman scattering for quantitative detection
of lung cancer biomarkers in superparticle @ MOF
structure [J]. Advanced Materials, 2018, 30
(5): 1702275.

[95] Paidi S K, Diaz P M, Dadgar S, et al. Label-free
Raman spectroscopy reveals signatures of radiation
resistance in the tumor microenvironment[J]. Cancer
Research, 2019, 79(8): 2054-2064.

[96] Zhang Y J, Zeng Q, Li L, et al. Characterization and
identification of lung cancer cells from blood cells
with label-free surface-enhanced Raman scattering
[J]. Laser Physics, 2019, 29(4): 045602.

[97] Sinica A, Brožáková K, Brůha T, et al. Raman
spectroscopic discrimination of normal and cancerous
lung tissues [J]. Spectrochimica Acta Part A:
Molecular and Biomolecular Spectroscopy, 2019,
219: 257-266.

[98] Song D L, Yu F, Chen S L, et al. Raman
spectroscopy combined with multivariate analysis to
study the biochemical mechanism of lung cancer
microwave ablation[J]. Biomedical Optics Express,
2020, 11(2): 1061-1072.

[99] Khan S, Ullah R, Shahzad S, et al. Optical
screening of nasopharyngeal cancer using Raman
spectroscopy and support vector machine[J]. Optik,
2018, 157: 565-570.

[100] Wu Q, Qiu S F, Yu Y, et al. Assessment of the
radiotherapy effect for nasopharyngeal cancer using

plasma surface-enhanced Raman spectroscopy technology[J]. Biomedical Optics Express, 2018, 9 (7): 3413-3423.

[101] Lin H, Zhou J, Wu Q, et al. Human blood test based on surface-enhanced Raman spectroscopy technology using different excitation light for nasopharyngeal cancer detection [J]. Iet Nanobiotechnology, 2019, 13(9): 942-945.

[102] Xue L L, Yan B, Li Y, et al. Surface-enhanced Raman spectroscopy of blood serum based on gold nanoparticles for tumor stages detection and histologic grades classification of oral squamous cell carcinoma [J]. International Journal of Nanomedicine, 2018, 13: 4977-4986.

[103] Ghosh A, Raha S, Dey S, et al. Chemometric analysis of integrated FTIR and Raman spectra obtained by non-invasive exfoliative cytology for the screening of oral cancer[J]. Analyst, 2019, 144 (4): 1309-1325.

[104] Jeng M, Sharma M, Sharma L, et al. Raman spectroscopy analysis for optical diagnosis of oral cancer detection[J]. Journal of Clinical Medicine, 2019, 8(9): 1313.

[105] Paraskevaidi M, Ashton K M, Stringfellow H F, et al. Raman spectroscopic techniques to detect ovarian cancer biomarkers in blood plasma [J]. Talanta, 2018, 189: 281-288.

[106] Morais C L M, Martin-Hirsch P L, Martin F. A three-dimensional principal component analysis approach for exploratory analysis of hyperspectral data: identification of ovarian cancer samples based on Raman microspectroscopy imaging of blood plasma[J]. Analyst, 2019, 144(7): 2312-2319.

[107] Zermeňo-Nava J D J, Martínez-Martínez M U, Rámirez-De-ávila A L, et al. Determination of sialic acid in saliva by means of surface-enhanced Raman spectroscopy as a marker in adnexal mass patients: ovarian cancer vs benign cases [J]. Journal of Ovarian Research, 2018, 11(1): 61.

[108] Viswanathan K, Soumya K, Gurusankar K, et al. Raman spectroscopic analysis of ovarian cancer tissues and normal ovarian tissues [J]. Laser Physics, 2019, 29(4): 045701.

[109] Carmicheal J, Hayashi C, Huang X, et al. Label-free characterization of exosome via surface enhanced Raman spectroscopy for the early detection of pancreatic cancer [J]. Nanomedicine: Nanotechnology, Biology and Medicine, 2019, 16:

88-96.

[110] Aubertin K, Desroches J, Jermyn M, et al. Combining high wavenumber and fingerprint Raman spectroscopy for the detection of prostate cancer during radical prostatectomy[J]. Biomedical Optics Express, 2018, 9(9): 4294-4305.

[111] Aubertin K, Trinh V Q, Jermyn M, et al. Mesoscopic characterization of prostate cancer using Raman spectroscopy: potential for diagnostics and therapeutics[J]. BJU International, 2018, 122(2): 326-336.

[112] Magalhães F L, Machado A M C, Paulino E, et al. Raman spectroscopy with a 1064-nm wavelength laser as a potential molecular tool for prostate cancer diagnosis: a pilot study[J]. Journal of Biomedical Optics, 2018, 23(12): 121613

[113] Lee W, Nanou A, Rikkert L, et al. Label-free prostate cancer detection by characterization of extracellular vesicles using Raman spectroscopy[J]. Analytical Chemistry, 2018, 90(19): 11290-11296.

[114] Correia N A, Batista L T A, Nascimento R J M, et al. Detection of prostate cancer by Raman spectroscopy: a multivariate study on patients with normal and altered PSA values [J]. Journal of Photochemistry and Photobiology B, 2020, 204: 111801.

[115] Qian H Y, Shao X G, Zhu Y J, et al. Surface-enhanced Raman spectroscopy of preoperative serum samples predicts Gleason grade group upgrade in biopsy Gleason grade group 1 prostate cancer[J]. Urologic Oncology, 2020, 38(6): 601.e1-601.e9.

[116] Feng X, Moy A J, Nguyen H T M, et al. Raman biophysical markers in skin cancer diagnosiss [J]. Journal of Biomedical Optics, 2018, 23 (5): 057002.

[117] Ferreira Lima A M, Daniel C R, Navarro R S, et al. Discrimination of non-melanoma skin cancer and keratosis from normal skin tissue *in vivo* and *ex vivo* by Raman spectroscopy [J]. Vibrational Spectroscopy, 2019, 100: 131-141.

[118] Garcia D V, da Silva Filho J I, Silveira L, Jr, et al. Analysis of Raman spectroscopy data with algorithms based on paraconsistent logic for characterization of skin cancer lesions [J]. Vibrational Spectroscopy, 2019, 103: 102929.

[119] Zhang X, Yu F, Li J, et al. Investigation on the cancer invasion and metastasis of skin squamous cell carcinoma by Raman spectroscopy[J]. Molecules,

2019, 24(11): 2059.

[120] O'Dea D, Bongiovanni M, Sykiotis G P, et al. Raman spectroscopy for the preoperative diagnosis of thyroid cancer and its subtypes: an *in vitro* proof-of-concept study[J]. Cytopathology, 2019, 30(1): 51-60.

[121] Liang X Z, Miao X C, Xiao W J, et al. Filter-membrane-based ultrafiltration coupled with surface-enhanced Raman spectroscopy for potential differentiation of benign and malignant thyroid tumors from blood plasma[J]. International Journal of Nanomedicine, 2020, 15: 2303-2314.

[122] Atkins C G, Buckley K, Blades M W, et al. Raman spectroscopy of blood and blood components[J]. Applied Spectroscopy, 2017, 71(5): 767-793.

[123] Perakis S, Speicher M R. Emerging concepts in liquid biopsies[J]. BMC Medicine, 2017, 15(1): 75.

[124] Siravegna G, Marsoni S, Siena S, et al. Integrating liquid biopsies into the management of cancer[J]. Nature Reviews Clinical Oncology, 2017, 14(9): 531-548.

[125] Xu X B, Li H F, Hasan D H, et al. Near-field enhanced plasmonic-magnetic bifunctional nanotubes for single cell bioanalysis[J]. Advanced Functional Materials, 2013, 23(35): 4332-4338.

[126] Nam W, Ren X, Tali S A S, et al. Refractive-index-insensitive nanolaminated SERS substrates for label-free Raman profiling and classification of living cancer cells[J]. Nano Letters, 2019, 19(10): 7273-7281.

[127] Wang J, Liang D W, Feng J, et al. Multicolor cocktail for breast cancer multiplex phenotype targeting and diagnosis using bioorthogonal surface-enhanced Raman scattering nanoprobes[J]. Analytical Chemistry, 2019, 91(17): 11045-11054.

[128] Lee J U, Kim W H, Lee H S, et al. Quantitative and specific detection of exosomal miRNAs for accurate diagnosis of breast cancer using a surface-enhanced Raman scattering sensor based on plasmonic head-flocked gold nanopillars[J]. Small, 2019, 15(17): 1804968.

[129] Kim S, Kim T G, Lee S H, et al. Label-free surface-enhanced Raman spectroscopy biosensor for on-site breast cancer detection using human tears [J]. ACS Applied Materials & Interfaces, 2020, 12 (7): 7897-7904.

[130] Bai X R, Wang L H, Ren J Q, et al. Accurate clinical diagnosis of liver cancer based on simultaneous detection of ternary specific antigens by magnetic induced mixing surface-enhanced Raman scattering emissions [J]. Analytical Chemistry, 2019, 91(4): 2955-2963.

[131] Tang R, Hu R, Jiang X H, et al. LHRH-targeting surface-enhanced Raman scattering tags for the rapid detection of circulating tumor cells[J]. Sensors and Actuators B, 2019, 284: 468-474.

[132] Lu D, Xia J, Deng Z, et al. Detection of squamous cell carcinoma antigen in cervical cancer by surface-enhanced Raman scattering-based immunoassay[J]. Analytical Methods, 2019, 11(21): 2809-2818.

[133] Xie M, Li F, Gu P L, et al. Gold nanoflower-based surface-enhanced Raman probes for pH mapping of tumor cell microenviroment[J]. Cell Proliferation, 2019, 52(4): e12618.

[134] Hong Y, Li Y Q, Huang L B, et al. Label-free diagnosis for colorectal cancer through coffee ring-assisted surface-enhanced Raman spectroscopy on blood serum[J]. Journal of Biophotonics, 2020, 13 (4): e201960176.

[135] Teng Y J, Ren Z Y, Zhang Y C, et al. Determination of prostate cancer marker Zn^{2+} with a highly selective surface-enhanced Raman scattering probe on liquid-liquid self-assembled Au nanoarrays [J]. Talanta, 2020, 209: 120569.

[136] Zhang X R, Liu C, Pei Y J, et al. Preparation of a novel Raman probe and its application in the detection of circulating tumor cells and exosomes [J]. ACS Applied Materials & Interfaces, 2019, 11 (32): 28671-28680.

[137] Zhang W, Jiang L M, Diefenbach R J, et al. Enabling sensitive phenotypic profiling of cancer-derived small extracellular vesicles using surface-enhanced Raman spectroscopy nanotags[J]. ACS Sensors, 2020, 5(3): 764-771.

[138] Reokrungruang P, Chatnuntawech I, Dharakul T, et al. A simple paper-based surface enhanced Raman scattering (SERS) platform and magnetic separation for cancer screening[J]. Sensors and Actuators B, 2019, 285: 462-469.

[139] Li L H, Liao M L, Chen Y F, et al. Surface-enhanced Raman spectroscopy (SERS) nanoprobes for ratiometric detection of cancer cells[J]. Journal of Materials Chemistry B, 2019, 7(5): 815-822.

[140] Nguyen T D, Song M S, Ly N H, et al. Nanostars on nanopipette tips: a Raman probe for quantifying

oxygen levels in hypoxic single cells and tumours [J]. Angewandte Chemie International Edition, 2019, 58(9): 2710-2714.

[141] Andreou C, Oseledchyk A, Nicolson F, et al. Surface-enhanced resonance Raman scattering nanoprobe ratiometry for detecting microscopic ovarian cancer via folate receptor targeting [J]. Journal of Visualized Experiments, 2019 (145): e58389.

[142] Niciński K, Krajczewski J, Kudelski A, et al. Detection of circulating tumor cells in blood by shell-isolated nanoparticle-enhanced Raman spectroscopy (SHINERS) in microfluidic device [J]. Scientific Reports, 2019, 9(1): 9267.

[143] Králová Z O, Oriňak A, Oriňaková R, et al. Electrochemically deposited silver detection substrate for surface-enhanced Raman spectroscopy cancer diagnostics[J]. Journal of Biomedical Optics, 2018, 23(7): 075002.

[144] Zhang K, Liu X J, Man B Y, et al. Label-free and stable serum analysis based on Ag-NPs/PSi surface-enhanced Raman scattering for noninvasive lung cancer detection [J]. Biomedical Optics Express, 2018, 9(9): 4345-4358.

[145] Zhang K, Hao C Y, Huo Y Y, et al. Label-free diagnosis of lung cancer with tissue-slice surface-enhanced Raman spectroscopy and statistical analysis[J]. Lasers in Medical Science, 2019, 34 (9): 1849-1855.

[146] Deng R, Yue J, Qu H X, et al. Glucose-bridged silver nanoparticle assemblies for highly sensitive molecular recognition of sialic acid on cancer cells via surface-enhanced Raman scattering spectroscopy [J]. Talanta, 2018, 179: 200-206.

[147] Chundayil Madathil G, Iyer S, Thankappan K, et al. A novel surface enhanced Raman catheter for rapid detection, classification, and grading of oral cancer[J]. Advanced Healthcare Materials, 2019, 8 (13): 1801557.

[148] Koo K M, Wang J, Richards R S, et al. Design and clinical verification of surface-enhanced Raman spectroscopy diagnostic technology for individual cancer risk prediction[J]. ACS Nano, 2018, 12(8): 8362-8371.

[149] Yang L, Zhen S J, Li Y F, et al. Silver nanoparticles deposited on graphene oxide for ultrasensitive surface-enhanced Raman scattering immunoassay of cancer biomarker[J]. Nanoscale,

2018, 10(25): 11942-11947.

[150] Brozek-Pluska B, Kopec M, Surmacki J. Surface-enhanced Raman spectroscopy analysis of human breast cancer via silver nanoparticles: an examination of fabrication methods[J]. Journal of Spectroscopy, 2018, 2018: 4893274.

[151] Si Y, Xu L, Wang N, et al. Target microRNA-responsive DNA hydrogel-based surface-enhanced Raman scattering sensor arrays for microRNA-marked cancer screening[J]. Analytical Chemistry, 2020, 92(3): 2649-2655.

[152] Xiang Y, Yang H R, Guo X Y, et al. Surface enhanced Raman detection of the colon cancer biomarker cytidine by using magnetized nanoparticles of the type $Fe_3O_4/Au/Ag$ [J]. Microchimica Acta, 2018, 185(3): 195.

[153] Cui X Y, Hu D Y, Wang C Y, et al. A surface-enhanced Raman scattering-based probe method for detecting chromogranin A in adrenal tumors [J]. Nanomedicine, 2020, 15(4): 397-407.

[154] Lin X L, Wang Y Y, Wang L N, et al. Interference-free and high precision biosensor based on surface enhanced Raman spectroscopy integrated with surface molecularly imprinted polymer technology for tumor biomarker detection in human blood [J]. Biosensors & Bioelectronics, 2019, 143: 111599.

[155] Dharmalingam P, Venkatakrishnan K, Tan B. Probing cancer metastasis at a single-cell level with a Raman-functionalized anionic probe [J]. Nano Letters, 2020, 20(2): 1054-1066.

[156] Keshavarz M, Kassanos P, Tan B, et al. Metal-oxide surface-enhanced Raman biosensor template towards point-of-care EGFR detection and cancer diagnostics[J]. Nanoscale Horizons, 2020, 5(2): 294-307.

[157] Miletić M, Aškrabić S, Rüger J, et al. Combined Raman and AFM detection of changes in HeLa cervical cancer cells induced by CeO_2 nanoparticles-molecular and morphological perspectives[J]. The Analyst, 2020, 145(11): 3983-3995.

[158] Hollon T C, Pandian B, Adapa A R, et al. Near real-time intraoperative brain tumor diagnosis using stimulated Raman histology and deep neural networks [J]. Nature Medicine, 2020, 26 (1): 52-58.

[159] Aljakouch K, Hilal Z, Daho I, et al. Fast and noninvasive diagnosis of cervical cancer by coherent

anti-stokes Raman scattering [J]. Analytical Chemistry, 2019, 91(21): 13900-13906.

[160] Zhang L L, Wu Y Z, Zheng B, et al. Rapid histology of laryngeal squamous cell carcinoma with deep-learning based stimulated Raman scattering microscopy[J]. Theranostics, 2019, 9(9): 2541-2554.

[161] Hollon T C, Lewis S, Pandian B, et al. Rapid intraoperative diagnosis of pediatric brain tumors using stimulated Raman histology [J]. Cancer Research, 2018, 78(1): 278-289.

[162] Shin K S, Francis A T, Hill A H, et al. Intraoperative assessment of skull base tumors using stimulated Raman scattering microscopy [J]. Scientific Reports, 9(1): 20392.

[163] Sarri B, Canonge R, Audier X, et al. Fast stimulated Raman and second harmonic generation imaging for intraoperative gastro-intestinal cancer detection[J]. Scientific Reports, 9(1): 10052.

[164] Yan S, Cui S S, Ke K, et al. Hyperspectral stimulated Raman scattering microscopy unravels aberrant accumulation of saturated fat in human liver cancer[J]. Analytical Chemistry, 2018, 90(11): 6362-6366.

[165] Huang K C, Li J J, Zhang C, et al. Multiplex stimulated Raman scattering imaging cytometry reveals lipid-rich protrusions in cancer cells under stress condition [J]. iScience, 2020, 23(3): 100953.

[166] Jin Q Q, Fan X L, Chen C M, et al. Multicolor Raman beads for multiplexed tumor cell and tissue imaging and *in vivo* tumor spectral detection[J]. Analytical Chemistry, 2019, 91(6): 3784-3789.

[167] Gong L, Zheng W, Ma Y, et al. Higher-order coherent anti-Stokes Raman scattering microscopy realizes label-free super-resolution vibrational imaging [J]. Nature Photonics, 2020, 14(2): 115-122.

[168] Li Z L, Li S W, Zhang S L, et al. Coherent Raman scattering microscopy technique and its biomedical applications[J]. Chinese Journal of Lasers, 2020, 47(2): 0207005.
李姿霖, 李少伟, 张思鹭, 等. 相干拉曼散射显微技术及其在生物医学领域的应用[J]. 中国激光, 2020, 47(2): 0207005.

[169] Zhang B H, Guo L, Yao L, et al. Rapid histological imaging using stimulated Raman scattering microscopy[J]. Chinese Journal of Lasers, 2020, 47(2): 0207018.
张博涵, 郭莉, 姚冽, 等. 受激拉曼散射显微技术用于快速无标记病理成像[J]. 中国激光, 2020, 47(2): 0207018.

[170] Davis R M, Kiss B, Trivedi D R, et al. Surface-enhanced Raman scattering nanoparticles for multiplexed imaging of bladder cancer tissue permeability and molecular phenotype [J]. ACS Nano, 2018, 12(10): 9669-9679.

[171] Zou Y X, Huang S Q, Liao Y X, et al. Isotopic graphene-isolated-Au-nanocrystals with cellular Raman-silent signals for cancer cell pattern recognition[J]. Chemical Science, 2018, 9(10): 2842-2849.

[172] Wu X X, Peng Y, Duan X M, et al. Homologous gold nanoparticles and nanoclusters composites with enhanced surface Raman scattering and metal fluorescence for cancer imaging[J]. Nanomaterials, 2018, 8(10): 819.

[173] Yarbakht M, Nikkhah M, Moshaii A, et al. Simultaneous isolation and detection of single breast cancer cells using surface-enhanced Raman spectroscopy[J]. Talanta, 2018, 186: 44-52.

[174] Liang D W, Jin Q Q, Yan N, et al. SERS nanoprobes in biologically Raman silent region for tumor cell imaging and *in vivo* tumor spectral detection in mice[J]. Advanced Biosystems, 2018, 2(12): 1800100.

[175] Zhang J, Liang L J, Guan X, et al. *In situ*, accurate, surface-enhanced Raman scattering detection of cancer cell nucleus with synchronous location by an alkyne-labeled biomolecular probe[J]. Analytical and Bioanalytical Chemistry, 2018, 410(2): 585-594.

[176] Zhang T, Qin Y T, Tan T W, et al. Targeted live cell Raman imaging and visualization of cancer biomarkers with thermal-stimuli responsive imprinted nanoprobes [J]. Particle & Particle Systems Characterization, 2018, 35(12): 1800390.

[177] Chang J, Zhang A, Huang Z C, et al. Monodisperse Au@Ag core-shell nanoprobes with ultrasensitive SERS-activity for rapid identification and Raman imaging of living cancer cells [J]. Talanta, 2019, 198: 45-54.

[178] Shi B W, Zhang B Y, Zhang Y Q, et al. Multifunctional gap-enhanced Raman tags for preoperative and intraoperative cancer imaging[J]. Acta Biomaterialia, 2020, 104: 210-220.

[179] Martinez Pancorbo P, Thummavichai K, Clark L, et al. Novel Au-SiO$_2$-WO$_3$ core-shell composite nanoparticles for surface-enhanced Raman spectroscopy with potential application in cancer cell imaging[J]. Advanced Functional Materials, 2019, 29(46): 1903549.

[180] Zhang Y Q, Liu Z Y, Thackray B D, et al. Intraoperative Raman-guided chemo-photothermal synergistic therapy of advanced disseminated ovarian cancers[J]. Small, 2018, 14(31): 1801022.

[181] Neuschmelting V, Harmsen S, Beziere N, et al. Dual-modality surface-enhanced resonance Raman scattering and multispectral optoacoustic tomography nanoparticle approach for brain tumor delineation[J]. Small, 2018, 14(23): 1800740.

[182] Wang J P, Sun J Y, Wang Y H, et al. Gold nanoframeworks with mesopores for Raman-photoacoustic imaging and photo-chemo tumor therapy in the second near-infrared biowindow[J]. Advanced Functional Materials, 2020, 30 (9): 1908825.

[183] Pal S, Ray A, Andreou C, et al. DNA-enabled rational design of fluorescence-Raman bimodal nanoprobes for cancer imaging and therapy [J]. Nature Communications, 10(1): 1926.

[184] Nicolson F, Andreiuk B, Andreou C, et al. Non-invasive *in vivo* imaging of cancer using surface-enhanced spatially offset Raman spectroscopy (SESORS)[J]. Theranostics, 2019, 9(20): 5899-5913.

[185] Nicolson F, Jamieson L E, Mabbott S, et al. Through tissue imaging of a live breast cancer tumour model using handheld surface enhanced spatially offset resonance Raman spectroscopy (SESORRS)[J]. Chemical Science, 2018, 9(15): 3788-3792.

[186] Song D L, Chen T M, Wang S, et al. Study on the biochemical mechanisms of the micro-wave ablation treatment of lung cancer by *ex vivo* confocal Raman microspectral imaging[J]. Analyst, 2020, 145(2): 626-635.

[187] Sitarz K, Czamara K, Bialecka J, et al. HPV infection significantly accelerates glycogen metabolism in cervical cells with large nuclei: Raman microscopic study with subcellular resolution [J]. International Journal of Molecular Sciences, 2020, 21(8): 2667.

[188] Brozek-Pluska B, Miazek K, Musial J, et al. Label-free diagnostics and cancer surgery Raman spectra guidance for the human colon at different excitation wavelengths[J]. RSC Advances, 2019, 9(69): 40445-40454.

[189] Morais C L M, Lilo T, Ashton K M, et al. Determination of meningioma brain tumour grades using Raman microspectroscopy imaging[J]. The Analyst, 2019, 144(23): 7024-7031.

[190] Feng X, Fox M C, Reichenberg J S, et al. Superpixel Raman spectroscopy for rapid skin cancer margin assessment [J]. Journal of Biophotonics, 2020, 13(2): e201960109.

[191] Feng X, Fox M C, Reichenberg J S, et al. Biophysical basis of skin cancer margin assessment using Raman spectroscopy [J]. Biomedical Optics Express, 2019, 10(1): 104-118.

[192] Abramczyk H, Imiela A, Brozek-Pluska B, et al. Aberrant protein phosphorylation in cancer by using Raman biomarkers [J]. Cancers, 2019, 11 (12): 2017.

[193] Placzek F, Cordero Bautista E, Kretschmer S, et al. Morpho-molecular *ex vivo* detection and grading of non-muscle-invasive bladder cancer using forward imaging probe based multimodal optical coherence tomography and Raman spectroscopy [J]. The Analyst, 2020, 145(4): 1445-1456.

[194] Sato S, Sekine R, Kagoshima H, et al. All-in-one Raman spectroscopy approach to diagnosis of colorectal cancer: analysis of spectra in the fingerprint regions [J]. Journal of the Anus, Rectum and Colon, 2019, 3(2): 84-90.

[195] Bury D, Morais C L M, Ashton K M, et al. *Ex vivo* Raman spectrochemical analysis using a handheld probe demonstrates high predictive capability of brain tumour status[J]. Biosensors, 2019, 9(2): 49.

[196] Liao C, Wang P, Huang C Y, et al. *In vivo* and *in situ* spectroscopic imaging by a handheld stimulated Raman scattering microscope[J]. ACS Photonics, 2018, 5(3): 947-954.

[197] Nicolson F, Jamieson L E, Mabbott S, et al. Multiplex imaging of live breast cancer tumour models through tissue using handheld surface enhanced spatially offset resonance Raman spectroscopy (SESORRS) [J]. Chemical Communications, 2018, 54(61): 8530-8533.

[198] Dai J H, He X, Li Z Y, et al. Fiber-optic Raman spectrum sensor for fast diagnosis of esophageal

cancer[J]. Photonic Sensors, 2019, 9(1): 53-59.

［199］ Varkentin A, Mazurenka M, Blumenröther E, et al. Trimodal system for *in vivo* skin cancer screening with combined optical coherence tomography-Raman and colocalized optoacoustic measurements[J]. Journal of Biophotonics, 2018, 11(6): e201700288.

［200］ Desroches J, Jermyn M, Pinto M, et al. A new method using Raman spectroscopy for *in vivo* targeted brain cancer tissue biopsy［J］. Scientific Reports, 8(1): 1792.

［201］ Han L M, Duan W J, Li X W, et al. Surface-enhanced resonance Raman scattering-guided brain tumor surgery showing prognostic benefit in rat models[J]. ACS Applied Materials & Interfaces, 2019, 11(17): 15241-15250.

［202］ Shams R, Picot F, Grajales D, et al. Pre-clinical evaluation of an image-guided *in situ* Raman spectroscopy navigation system for targeted prostate cancer interventions ［J］. International Journal of Computer Assisted Radiology and Surgery, 2020, 15(5): 867-876.

［203］ McGregor H C, Short M A, Lam S, et al. Development and *in vivo* test of a miniature Raman probe for early cancer detection in the peripheral lung ［J］. Journal of Biophotonics, 2018, 11 (11): e201800055.

［204］ Lin D, Qiu S F, Huang W, et al. Autofluorescence and white light imaging-guided endoscopic Raman and diffuse reflectance spectroscopy for *in vivo* nasopharyngeal cancer detection ［J］. Journal of Biophotonics, 2018, 11(4): e201700251.

［205］ Xu H, Zhu Y K, Lu Y F, et al. Development and biomedical application of Raman probe[J]. Laser & Optoelectronics Progress, 2019, 56(11): 110005.
徐浩, 朱勇康, 陆燕飞, 等. 拉曼探头的发展及其生物医学应用[J]. 激光与光电子学进展, 2019, 56 (11): 110005.